Opt Quant Electron (2015) 47:375–385
DOI 10.1007/s11082-014-9919-x

Effect of hole mobilities through the emissive layer on space charge limited currents of phosphorescent organic light-emitting diodes

Yang Luo · Yu Duan · Ping Chen · Yi Zhao

Received: 7 December 2013 / Accepted: 18 March 2014 / Published online: 3 April 2014

Abstract In this letter, we used space charge limited current measurements to evaluate the hole mobilities of candidate host materials with or without doped phosphorescent guests through a study of "hole only" devices. We found different impacts to hole mobility in each material when the dopant concentration changes. We postulated that the guest/host energy level matching in the light emissive layer plays an important role in the performance of organic light emitting devices. A number of white organic light emitting devices were designed to prove the supposition. Using guest/host energy level matching a device was fabricated which demonstrated higher efficiency, lower efficiency roll-off and lower driving voltage compared to a non-level-matched device.

Keywords Hole mobilities · Space charge limited currents · Phosphorescent organic light-emitting diodes

1 Introduction

Organic materials that can be fabricated by simple processing techniques and that display excellent electrical performance are vital to the future of semiconductor electronics (Burrows 1998; D'Andrade and Forrest 2004). The charge-carrier mobility of an organic semiconducting material is a key selection criterion for solid-state devices such as organic light-emitting diodes (OLEDs) (Li et al. 2008), organic photovoltaic diodes (OPVs) (Dai et al. 2008), and organic field-effect transistors (OTFTs) (Orgiu 2011). Currently, one of the most effective and

Y. Luo · Y. Duan (✉) · P. Chen · Y. Zhao
State Key Laboratory on Integrated Optoelectronics, College of Electronics Science and Engineering, Jilin University, 2699 Qianjin Street, Changchun 130012, People's Republic of China
e-mail: duanyu@jlu.edu.cn

Y. Luo
Key Laboratory of Excited State Processes, Changchun Institute of Optics, Fine Mechanics and Physics, Chinese Academy of Sciences, 3888 Dong Nanhu Road, Changchun 130012, People's Republic of China

widely used methods for measuring the mobility of organic semiconductors is the time-of-flight (TOF) measurement (Chen 2001). For TOF measurements, a given voltage is applied to a test sample and a pulsed light illuminates one end to generate carriers. As charge carriers drift to the other electrode, the resulting photocurrent is monitored. The mobility of charge carriers is calculated from the changes in the current. However, TOF is only applicable to devices whose effective thickness is greater than 1 μm. In general, the electrical and optical properties of organic semiconductors are dependent on their thickness (Azuma et al. 2006), and hence mobility measurements should be carried out in organic thin film test sample whose thickness is comparable to those in practical devices. Space charge limited current (SCLC) measurements (Meng 2008) can be used to determine charge carrier mobility in organic semiconducting thin films whose thickness is easily customized. Thus, it is more relevant to perform SCLC measurements on OLEDs and OPVs to determine the field-dependent mobilities.

In this letter, we have conducted a study of "hole-only" devices, using SCLC measurements to evaluate the hole mobilities of four candidate hosts: (1) N,N'-bis-(1-naphthyl)-N,N'-diphenyl-1,1′-biphenyl-4, 4′-diamine (NPB); (2) 4,4′,4″-tris(3-methylphenylphenylamino)-triphenylamine (m-MTDATA); (3) 4,4′-bis(carbazol-9-yl)biphenyl (CBP); and (4) bis(2-methyl-8-quinolinato)-4-phenylphenolate (Balq). By introduction of a MoO_3 interlayer between the organic materials and the electrodes, the zero-field mobilities and field-dependent factors of each of the four materials have been determined, and the evolution of hole mobilities with respect to the bias voltage has been characterized. In conventional electrophosphorescent OLEDs, the exciton formation zone is located in the emission layer (EML) adjacent to one or both adjacent carrier transport layers. This pileup of excitons at the EML can lead to enhanced triplet–triplet annihilation (Cheng 2006; Baldo et al. 2000). Here, we investigated the hole mobility of red EMLs and then employed the red EMLs with higher hole mobility in white OLEDs (WOLEDs); this higher mobility yields a broad distribution of excitons across the EML which results in a higher efficiency.

2 Theoretical background

A prerequisite for using SCLC for mobility measurements is an Ohmic contact to the sample for current injection. However, the electrodes in common use do not provide Ohmic contacts. By altering the interface material or inserting a buffer layer between the organic layer and the electrode, we can form quasi-ohmic contacts, which allow us to utilize SCLC for mobility determination. In our devices, we inserted a thin MoO_x film between the organic layer and the electrodes; this ensures effective quasi-ohmic injection and extraction of charge carriers through a very thin space–charge layer (Meng 2008). Moreover, the nearly symmetric device architecture eliminates the built-in-potential and interface effects usually observed in single-carrier devices without doped charge transport layers (Yasuda et al. 2002; Kim and Jang 2006; Chu and Song 2007), since the Fermi level in the organic layers is determined by the organic-electrode interfaces. The typical current–voltage relationship of a metal/organic/metal device can be split into three distinct regions and it enters the region accessible to SCLC measurements when the test sample is under high bias voltage (Carbone et al. 2009). At this point the number of electrons or holes injected into the sample per second is larger than can be accepted by space. The excess electrons or holes form negative space charges which result in an electric field and reduce the rate of electron or hole emission from the electrode. In this high-voltage condition, the current drift through the device is determined by the carrier mobility of the organic material, ignoring the impact of traps and bias voltage. The Poisson equation (1) and continuity equation (2) are solved analytically to obtain the relation between the current density J and bias voltage V (Eq. 3).

$$\frac{\varepsilon_0 \varepsilon_r}{e} \frac{dE(x)}{d(x)} = \rho(x) \tag{1}$$

$$j = \rho(x) e \mu E(x) \tag{2}$$

$$j = \frac{9}{8} \varepsilon_0 \varepsilon_r \mu \frac{V^2}{L^3} \tag{3}$$

In Eq. (2), ρ(x) is the charge density and E(x) is the electric field, both a function of distance through the slab. V is the bias voltage, L is the thickness of the sample, μ is the carrier mobility, e is the elementary charge and ε_0 and ε_r are the permittivity of free space and relative permittivity of the organic material, respectively. Typically, the value of ε_r used for the common organic semiconductors we studied is 3. This conclusion was first published by Mott and Gurney to determine the mobility of a material (Mott and Gurney 1948). However it has been discussed that the carrier mobility of organic materials always exhibits a strong electric field dependence which can be described by the Poole–Frenke equation (4).

$$\mu(E) = \mu_0 exp(\gamma \sqrt{E}) \tag{4}$$

In this equation, μ_0 is the zero-field mobility and γ is the field-dependent factor. From a combination of Eqs. (3) and (4), the dependent SCLC can be easily expressed by the equations below:

$$j = \frac{9}{8} \varepsilon_0 \varepsilon_r \mu_0 \frac{E^2}{L} exp(\gamma \sqrt{E}) \tag{5}$$

$$ln\left(\frac{J}{E^2}\right) = ln\left(\frac{9}{8} \frac{\varepsilon_r \varepsilon_0 \mu_0}{L}\right) + \gamma \sqrt{E} \tag{6}$$

Equation (6) shows a linear relationship between $ln\left(\frac{J}{E^2}\right)$ and $\sqrt{E}$. If we plot the functional image of $ln\left(\frac{J}{E^2}\right)$ corresponding to $\sqrt{E}$, we can calculate the zero-field mobility μ_0 and field-dependent factor γ from the intercept and slope, respectively. From there, the field-dependent carrier mobility under a given voltage can be calculated using Eq. (4).

3 Experiment results and discussion

The hole-only architecture we designed is glass/ITO/MoO_x(10 nm)/organic material (120 nm)/ MoO_x(10 nm)/Al(50 nm), where the organic material is one of the four candidate hosts (NPB, m-MTDATA, CBP, and Balq). The glass substrate was cleaned with acetone and alcohol and cleaned ultrasonically with de-ionized water. The devices were prepared by vacuum vapor deposition (4×10^{-4} Pa). The deposition rates of the thin films were controlled through feedback from a IL-400 film thickness monitor, and the current–voltage (I–V) characteristics were measured by a computer-controlled programmable Keithley 2400 DC source meter. The electroluminescence (EL) spectra, brightness and CIE color space coordinates were recorded with Spectra Scan PR650. All the tests were conducted under atmospheric conditions.

Figure 1 shows the current density–voltage (J–V) characteristics of the four devices. It shows two distinct regions, at low ($\sim 10^4$–10^5 V cm^{-1}) and high ($\sim 10^5$–10^6 V cm^{-1}) biases, which we interpreted as the trap charge limited current region and the SCLC region, respectively. In order to confirm this view, we fitted the J–V^2 relationships of the four materials. The results are shown in Fig. 2. As we can see, the linear relation between J and V^2 could be observed at high bias voltage. All the J–V characteristics could be described by $J \propto V^2$

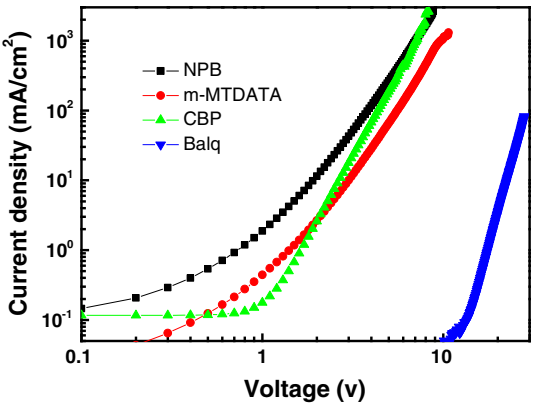

Fig. 1 J–V characteristics of the four hole-only devices

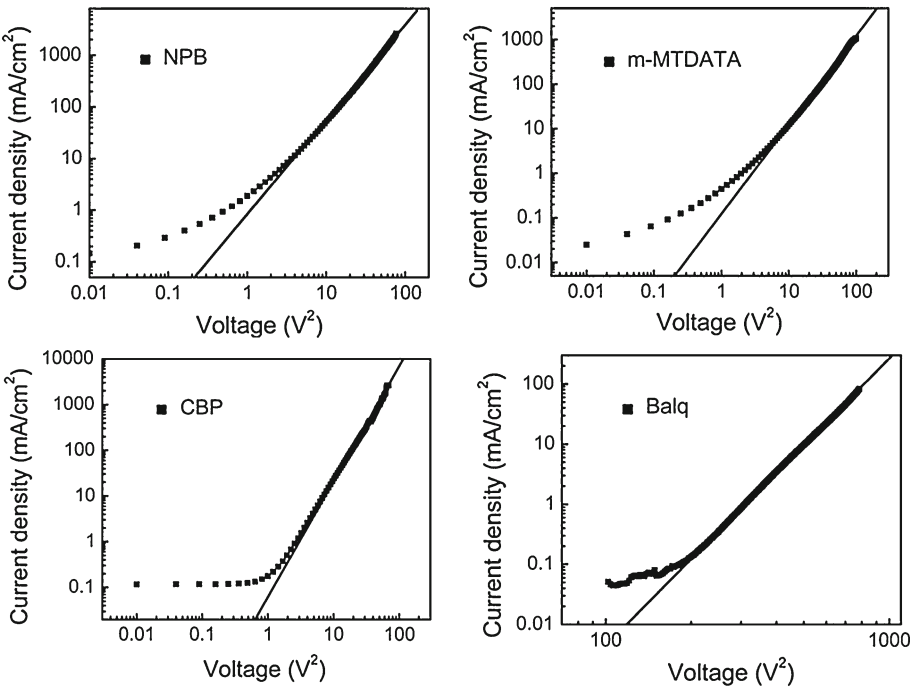

Fig. 2 J–V^2 characteristics of the four hole-only devices. *Black lines* are linear fits to the high-bias SCLC regions

in this region. This supports our premise that the sample enters the trap-free SCLC region when the bias voltage is high enough (Chung et al. 2008).

The current density data of the four devices at high biases are extracted to plot the linear relation of $ln\left(\frac{J}{E^2}\right)$ to$\sqrt{E}$, as shown in Fig. 3. The fitted lines are in good agreement with the experimental data. The intercepts and slopes are extracted from the fit and substituted into Eq. (6) to obtain the zero-field hole mobility μ_0 and field-dependent factor γ. The results are collected in Table 1. By comparing these results, we find that the zero-field hole mobility of Balq is about six orders of magnitude smaller than that of CBP or m-MADATA. The zero-

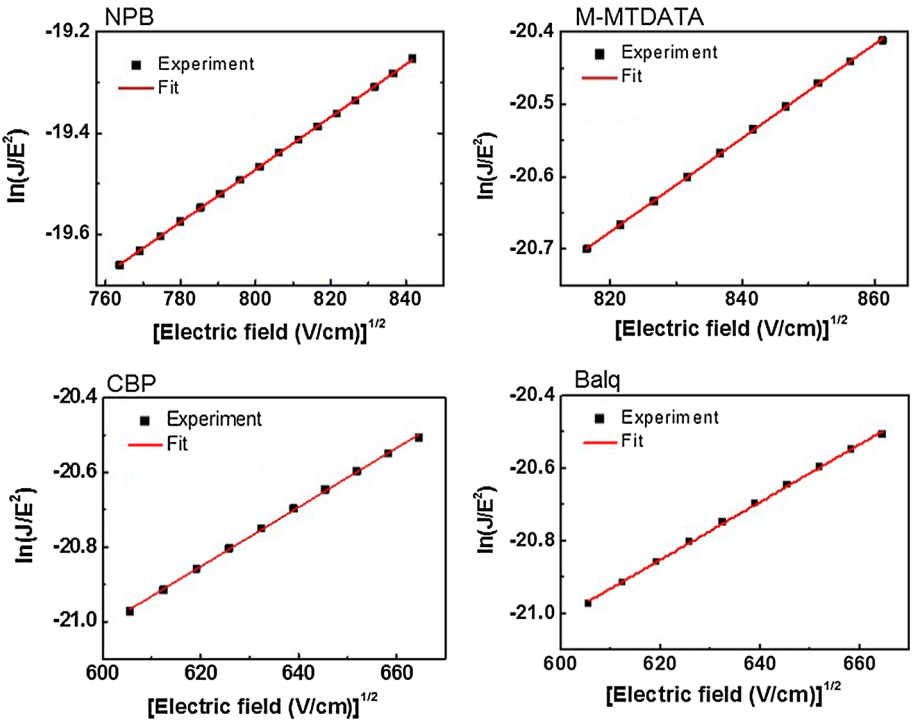

Fig. 3 The experimental data (*black squares*) and fitted curves (*red lines*) of $ln\left(\frac{J}{E^2}\right)$ corresponding to $\sqrt{E}$ of the four devices

Table 1 The zero-field mobilities μ_0 and field-dependent factors γ calculated for the four devices

Material	μ_0 ($cm^2\,V^{-1}\,s^{-1}$)	γ $(cm\,V)^{1/2}$
NPB	2.23×10^{-3}	0.00518
m-MTDATA	2.06×10^{-4}	0.00649
CBP	2.57×10^{-4}	0.00794
Balq	1.43×10^{-10}	0.00995

field hole mobility and field-dependent factors we fitted were substituted into Eq. (4) to show the evolution of hole mobilities with respect to an increasing electric field (Fig. 4). These data determined by SCLC measurement have the same order of magnitude and similar trends to measurements from previous reports (Matsusue et al. 2005; Tse et al. 2006; Nakayama et al. 2009).

According to the previous study, doping phosphorescent dyes in hosts may impact those hosts charge mobility (Park et al. 2008; Parshin et al. 2006). To acquire detailed information about charge transport in the doped hosts, we fabricated unipolar (hole-only) devices with different host materials according to the following scheme: glass/ITO/MoO_x(10 nm)/host: dopant(120 nm)/MoO_x(10 nm)/Al(50 nm). Host stands for NPB, m-MTDATA, CBP, and Balq, respectively, and the dopant is bis(1-phenyl-isoquinoline)(Acetylacetonato)iridium(III), $Ir(piq)_2(acac)$. Devices with doping concentrations of 0, 1, 5 and 10 %wt were fabricated for each host material. The field-dependent hole mobilities of these hosts with different dopant concentrations are shown in Fig. 5. As we can see, changing the dopant concentration of

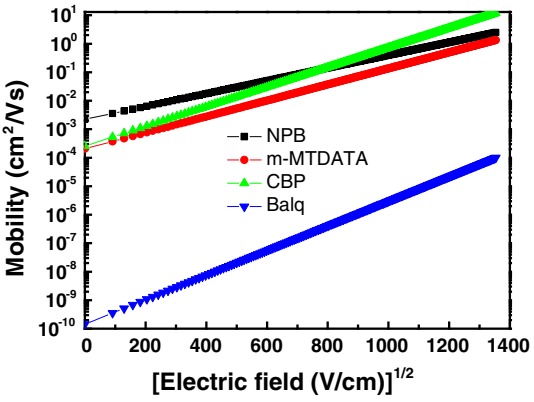

Fig. 4 Hole mobility versus electric field for the four host materials

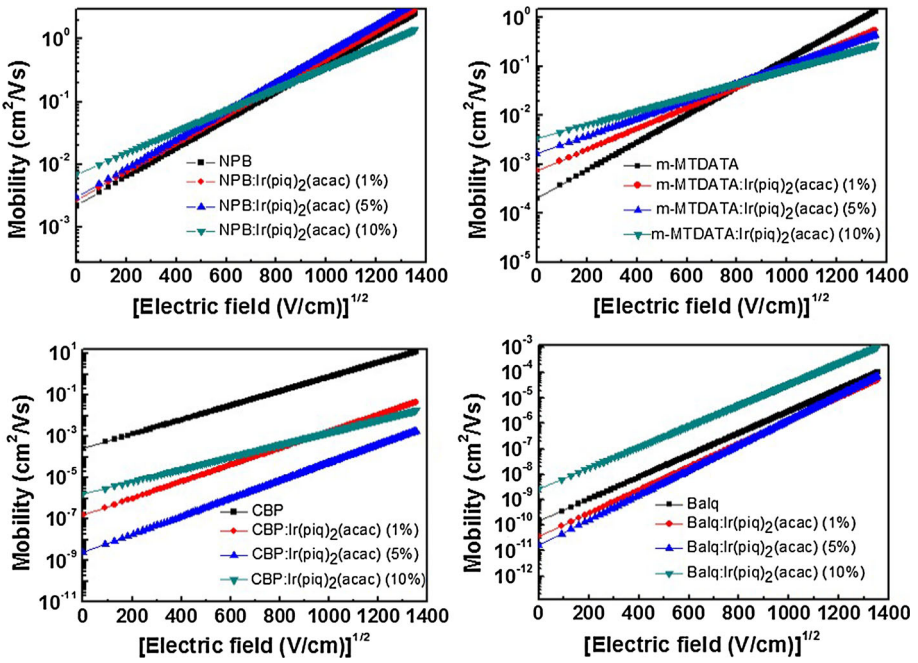

Fig. 5 Hole mobility versus electric field for the four host materials with different dopant concentrations

$Ir(piq)_2(acac)$ had different effects on the hole mobilities of each host. For NPB and m-MTDATA, the effects are limited. The hole mobilities have remained within an order of magnitude as the dopant concentration grows. In contrast, the impacts are obvious in CBP and Balq. The hole mobilities change by more than two orders of magnitude when the dopant concentration changes. It also can be observed that when doping $Ir(piq)_2(acac)$ into CBP or Balq with lower doping concentration (<5 %wt), the hole mobility decreases significantly since holes undergo deep trapping at the HOMO level of $Ir(piq)_2(acac)$. However, the hole mobility starts to increase when the doping concentration is increased to 10 %.

In order to clearly understand these effects, the energy levels for each host and the dopant are clearly given in Fig. 6. As we can see, the HOMO levels of NPB and m-MTDATA are

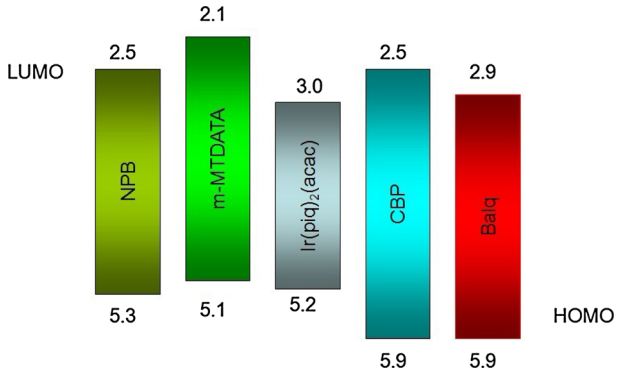

Fig. 6 The structure of the energy levels from HOMO to LUMO for each of the organic material hosts and the dopant

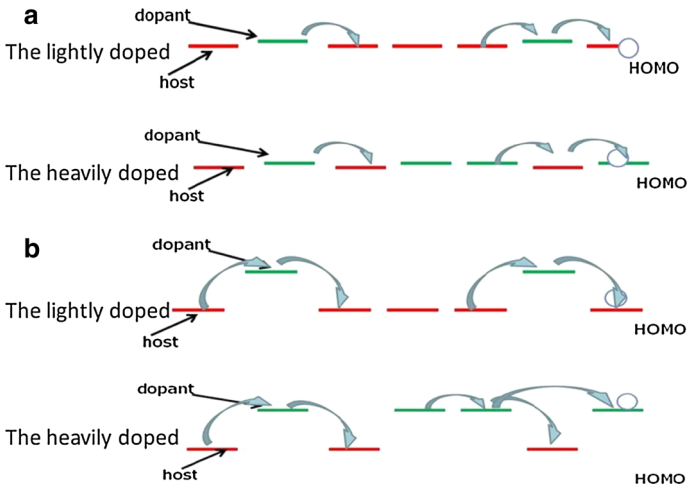

Fig. 7 The hole-transports models of phosphorescent doped hosts. **a** NPB or m-MTDATA doped with Ir(piq)2(acac), **b** CBP or Balq doped with Ir(piq)2(acac)

similar to that of $Ir(piq)_2(acac)$($<$0.2 eV). In contrast, the HOMO levels of CBP and Balq are much lower than $Ir(piq)_2(acac)$($>$0.2eV). Two different kind of hole-transport models are shown in Fig. 7. In the first case (Fig. 7a), no obvious trap iss formed when holes are transporting between host and dopant because of the match in the levels of host and dopant HOMOs. Therefore, the increase of doping concentration does not affect hole mobility obviously. On the other hand, traps are formed when doping $Ir(piq)_2(acac)$ into CBP or Balq because of the level mismatch between host and dopant. Therefore, with lower doping concentration ($<$5 %wt), the hole mobility decreases significantly since holes undergo deep trapping at the HOMO level of $Ir(piq)_2(acac)$. However, holes hopping directly through dopant HOMOs occurs when doping concentration increases further (Fig. 7b). This kind of hopping gets easier as the doping concentration grows. So the hole mobility increases when the doping concentration is increased to 10 %.

Based on the results discussed above, we further conjectured that the match of host and dopant energy level in the light emissive layer plays an important role in the performance

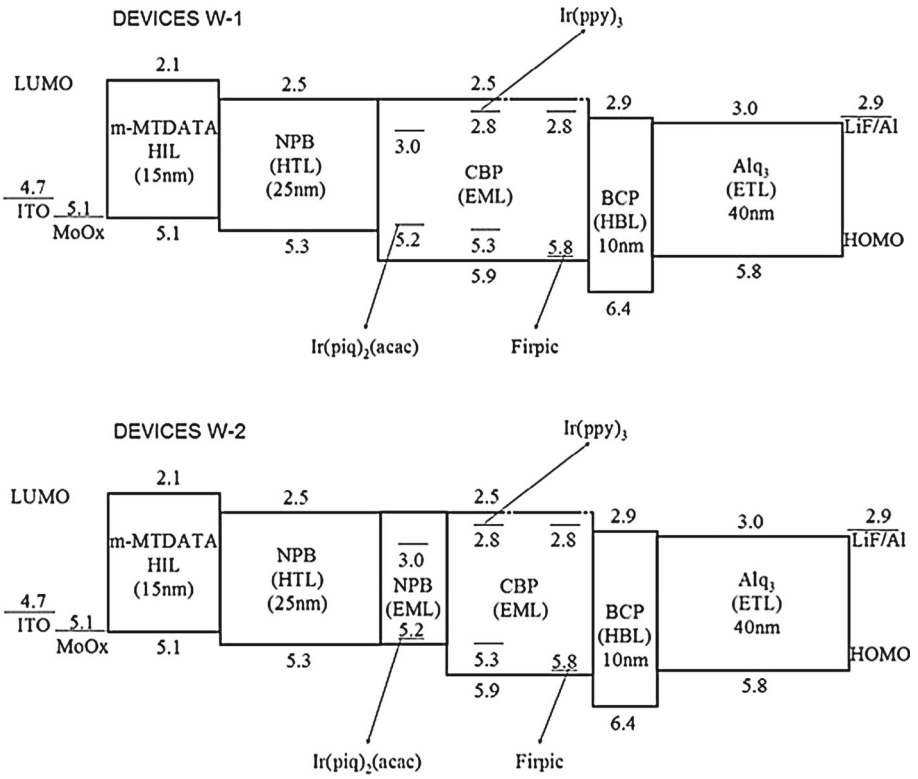

Fig. 8 The schematic the energy levels of the WOLEDs with two different REML host materials

of OLEDs. The hole mobility is larger when the gap between the HOMOs of the host and dopant is <0.2 eV. A higher hole mobility through the emissive layer results in a wider carrier distribution and a better carrier balancing, which in turn lead to better performance of OLEDs. On the other hand, a large mismatch between the HOMOs of the host and dopant leads to a lower hole mobility. The performance of an OLED may not be good in this condition. To prove this supposition, we designed two groups of WOLEDs using different hosts in the red emitting layer. Figure 8 shows the structure of the devices, the energy level diagram of the materials used in the work, and their LUMO and HOMO values. In the group of devices labelled W-1, a 15-nm CBP layer doped with x %wt (x = 1, 3, 7, and 10) Ir(piq)$_2$(acac), a 10-nm CBP layer doped with 4 % fac-tris(2-phenylpyridine)iridium(III) (Ir(ppy)$_3$), and a 15-nm CBP doped with 9 % iridium(III)bis[(4,6-difluorophenyl)-pyridinato-N,C2′] picolinate (FIrpic) were used as the R,G and B EMLs, respectively. A 3 nm CBP layer was placed between each pair of EMLs. In the group of devices labelled W-2, the red EML was replaced with a 15-nm NPB layer doped with y %wt (y = 1, 3, 7, and 10) Ir(piq)$_2$ (acac).

Figure 9 shows the normalized EL spectra of the W1 and W2 devices at 30 mA/cm^2. Three EL peaks can be verified from Ir(piq)$_2$(acac) at $\lambda \sim 625$ nm, Ir(ppy)$_3$ at $\lambda \sim 500$ nm, and FIrpic at $\lambda \sim 470$ nm, resulting in white light emission. Figure 10 gives the variation of the CIE 1931 chromaticity coordinates of those WOLEDs at a luminance of 1,000 cd/m^2. Devices in group W-2, based on NPB doped with Ir(piq)$_2$(acac), show less shift of chromaticity coordinates with increasing doping concentration compared to devices in group

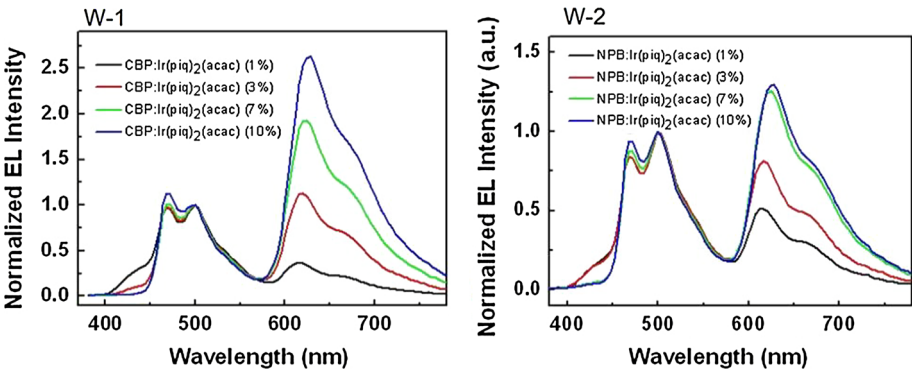

Fig. 9 The normalized EL spectra at 30 mA/cm^2 of WOLEDs CBP (*left*) and NBP (*right*) as the host materials and with varying dopant concentrations

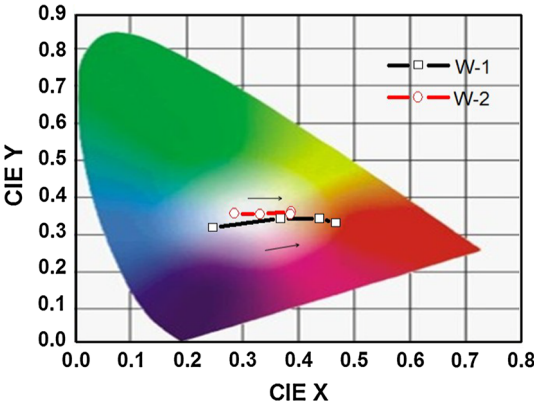

Fig. 10 The variation of the CIE 1931 chromaticity coordinates of the two groups WOLEDs (W1, *red*, and W2, *black*) at 1,000 cd/m^2 for increasing dopant concentration (direction marked by *arrows*)

W-1. Because of more stable hole mobility with varying guest content in NPB:Ir(piq)$_2$(acac) than in CBP:Ir(piq)$_2$(acac), W-2 devices are less sensitive to red emissive layer doping concentration than W-1 devices. When the doping concentration of Ir(piq)$_2$(acac) is 3 %wt, the driving voltage of the W-2 device at the luminance of 100 cd/m^2 are obtained at least 0.8 V lower, compared with the W-1 device. The external quantum efficiencies (EQEs) for these two devices are shown in Fig. 11. The maximum EQEs obtained are 3.4 % at 6.76 mA/cm^2 and 330 cd/m^2 (W-1), 3.85 % at 4.81 mA/cm^2 and 320 cd/m^2 (W-2). A lower roll-off of EQEs of W-2 (19 % from 10 to 100 mA/cm^2) compared to W-1 (33 % from 10 to 100 mA/cm^2) can be also observed. This phenomenon is due to the fact that a higher hole mobility through the emissive layer results in a wider carrier distribution and a better carrier balancing. The better balancing spreads the recombination zone, reducing the pileup of excitons at a single EML. In addition, it also alleviates the problem of free carriers around the emitters and restrains the triplet–triplet quenching effect (Duan 2010).

4 Conclusions

In conclusion, the hole mobilities of host materials with or without varying doping guest content have been determined by SCLC measurements. We found different impacts on hole

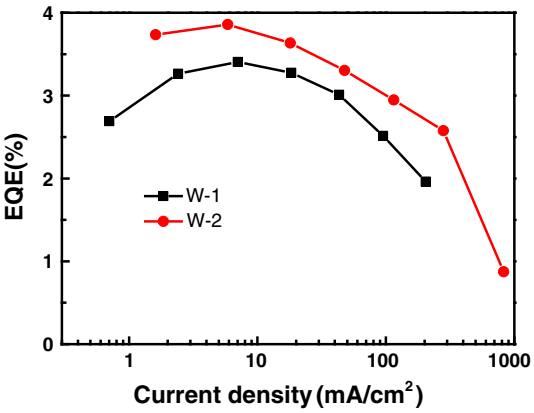

Fig. 11 The EQEs of the 3 %wt doped devices with CBP (*black*) and NBP (*red*) hosts as a function of current density

mobility from changes in the dopant concentration. The match of host and dopant energy level in light emissive layer plays an important role in the performance of organic light emitting devices (OLEDs) was further conjectured. This work contributes to the understanding of the significant role of guest/host energy level matching on the carrier mobilities in the emissive layer, and to the illumination of the possible mechanisms that govern the effects of the dopant concentration on multilayer electrophosphorescent WOLEDs. Finally, white organic light emitting devices were fabricated that demonstrated a higher efficiency, a lower roll-off of efficiency and a lower driving voltage than those of a similar device with less optimal guest/host level matching. Further improvements are possible for phosphorescent WOLEDs by employing such guest/host engineering simultaneously in Red, Green and Blue layers, and we plan to explore this in future experiments.

Acknowledgments This work was supported by Program of international science and technology cooperation (2014DFG12390), National High Technology Research and Development Program of China (Grant No. 2011AA03A110), Ministry of Science and Technology of China (Grant No. 2010CB327701, 2013CB834802), the National Natural Science Foundation of China (Grant Nos. 61275024, 61274002, 61275033, 6137706 and 41001302), Scientific and Technological Developing Scheme of Jilin Province (Grant No. 20140101204JC, 20140520071JH), Scientific and Technological Developing Scheme of Changchun (Grant No.13GH02), the Opened Fund of the State Key Laboratory on Integrated Optoelectronics No. IOSKL2012KF01.

References

Azuma, H., Asada, K., Kobayashi, T., Naito, H.: Fabrication of α- and β-phase poly(9,9-dioctylfluorene) thin films. Thin Solid Film **509**, 182–184 (2006)

Baldo, M.A., Adachi, C., Forrest, S.R.: Transient analysis transient analysis of organic electrophosphorescence. II. of triplet-triplet annihilation. Phys. Rev. B **62**, 10967–10977 (2000)

Burrows, P.E., et al.: Light emitting devices using vacuum deposited organic thin films. Thin Solid Films **331**, 101–105 (1998)

Carbone, A., Pennetta, C., Reggiani, L.: Substrate-dependent interface composition and charge transport in films for organic photovoltaics. Appl. Phys. Lett. **95**, 233303 (2009)

Chen, Z., et al.: Influence of sensitizer on organic electroluminescence. J. Appl. Phys. **89**, 7895–7898 (2001)

Cheng, G., et al.: White organic light-emitting devices with a phosphorescent multiple emissive layer. Appl. Phys. Lett. **89**, 043504 (2006)

Chu, T.Y., Song, O.K.: Hole mobility of *N,N*-bis (naphthalen-1-yl)-*N,N*-bis (phenyl) benzidine investigated by using space-charge-limited currents. Appl. Phys. Lett. **90**, 203512 (2007)

Chung, D.S., Lee, D.H., Yang, C.: Origin of high mobility within an amorphous polymeric semiconductor: space-charge-limited current and trap distribution. Appl. Phys. Lett. **93**, 033303 (2008)

Dai, J.G., Jiang, X.X., Wang, H.B., Yan, D.H.: Organic photovoltaic cell employing organic heterojunction as buffer layer. Thin Solid Films **516**, 3320–3323 (2008)
D'Andrade, B.W., Forrest, S.R.: White organic light-emitting devices for solid-state lighting. Adv. Mater. **16**, 1585–1595 (2004)
Duan, Y., et al.: High-efficiency red phosphorescent electroluminescence devices based on mixed p/n host matrices. Opt. Lett. **35**, 3174–3176 (2010)
Kim, S.H., Jang, J.: Relationship between indium tin oxide surface treatment and hole injection in C60 modified devices. Appl. Phys. Lett. **89**, 253501 (2006)
Li, H., Wang, N., Liu, X.: Optical and electrical properties of vanadium doped indium oxide thin films. Opt. Express. **16**, 194–199 (2008)
Matsusue, N., Suzuki, Y., Naito, H.: Charge carrier transport in neat thin films of phosphorescent iridium complexes. Jpn. J. Appl. Phys. **44**, 3691–3694 (2005)
Meng, Y., et al.: Effective hole-injection layer for non-doped inverted top-emitting organic light-emitting devices. Microelectron. J. **39**, 723–726 (2008)
Mott, N.P., Gurney, R.W.: Electronic Processes in Ionic Crystals. Oxford University Press, London 275–278 (1948)
Nakayama, K.I., Ishikawa, M., Yokoyama, M.: Improvement in mobility and stability of n-type organic field-effect transistors with a hole transporting interfacial layer. Appl. Phys. Exp. **2**, 021501 (2009)
Orgiu, E., et al.: Analysis of the hysteresis in organic thin-film transistors with polymeric gate dielectric. Org. Electron. **12**, 477–485 (2011)
Park, T.J., Jeon, W.S., Kwon, J.H.: Efficient simple structure phosphorescent organic light emitting devices with narrow band gap fluorescent hosts. Proc. SPIE **7051**, R0510 (2008)
Parshin, M.A., Ollevier, J., der Auweraer, M.V.: Charge carrier mobility in CBP films doped with Ir(ppy)3. Proc. SPIE **6192**, A1922 (2006)
Tse, S.C., Tsang, S.W., So, S.K.: Nearly ohmic injection contacts from PEDOT:PSS to phenylamine compounds with high ionization potentials. Proc. SPIE **6333**, P3331 (2006)
Yasuda, T., Yamaguchi, Y., Zou, D.C., Tsutsui, T.: Carrier mobilities in organic electron transport materials determined from space charge limited current. Jpn. J. Appl. Phys. **41**, 5626–5629 (2002)